Polymer 302 (2024) 127065

Contents lists available at ScienceDirect

Polymer

journal homepage: www.elsevier.com/locate/polymer

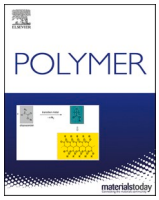

In-situ hybridization of an epoxy resin using polyurethane and MXene nanoplatelets for thermally stable nanocomposites with improved strength and toughness

Yi Hu [a,b,d], Junzhen Chen [a,d], Guoyu Yang [a,d], Yujun Li [a,d], Ming Dong [b], Qi Li [c], Hongna Yuan [b], Han Zhang [b], Nicola M. Pugno [b,e], Jianjun Jiang [a,d,**], Dimitrios G. Papageorgiou [b,*]

[a] School of Mechanical Engineering, Northwestern Polytechnical University, Xi'an, 710072, PR China
[b] School of Engineering and Materials Science, Queen Mary University of London, London, E1 4NS, UK
[c] Department of Chemistry, School of Physical and Chemical Sciences, Queen Mary University of London, London, E1 4NS, UK
[d] Shaanxi Engineering Research Center for Digital Manufacturing, Xi'an, 710072, PR China
[e] Laboratory for Bioinspired, Bionic, Nano, Meta, Materials & Mechanics, Department of Civil, Environmental and Mechanical Engineering, University of Trento, Via Mesiano, 77, 38123, Trento, Italy

ARTICLE INFO

Keywords:
MXene
PU
Nanocomposite
Strength
Fracture toughness

ABSTRACT

A novel ternary composite system has been developed by combining MXene nanoplatelets with pre-polyurethane (PU) and an epoxy (EP) resin through *in-situ* polymerization and solution blending. Our approach aims to enhance the strength and toughness of the EP matrix while maintaining its thermal stability. The strong compatibility between isocyanate-terminated PU and hydroxyl-terminated MXene with the resin was demonstrated through chemical grafting and hydrogen bonding processes. In this ternary composite, significant improvements were observed, including a 32 % increase in tensile strength, a 46.4 % increase in flexural strength, and a 13.4 % increase in fracture toughness, even at very low filler contents of 0.05 wt% for MXene and 1 wt% for PU. A thorough examination of the fractured surfaces revealed the underlying mechanisms responsible for the improved strength and toughness. These mechanisms involve a transition from a brittle to a ductile fracture mode, which can be attributed to the combined effects of thermoplastic toughness, strong chemical bonding between PU and EP, and crack-anchoring and bridging effects facilitated by MXene nanoplatelets. The results presented herein are relevant to a wide range of applications in aerospace, automotive, electronics and various other industries where durability and thermomechanical performance of materials are critical.

1. Introduction

Epoxy (EP) composites are widely used in various industries due to their excellent mechanical properties, chemical resistance, and stability. Nevertheless, a number of observed difficulties have been known to restrict their applications. One significant issue is their inability to withstand impacts and cyclic loads, making brittleness a concern that needs to be addressed urgently [1–4]. Brittleness hinders energy dissipation, leading to the initiation and propagation of cracks over time, which can ultimately result in catastrophic failures, posing risks to human lives and properties. Carbon fiber reinforced polymer (CFRP) composites, where epoxy resins are predominantly used as the matrix, have emerged as prime contenders for aerospace and automotive components. However, the brittleness inherent to epoxy resins also constrains the broad-scale integration of CFRP composites.

In light of these significant challenges, several strategies have been employed to enhance the toughness and thus strength and ductility of epoxy composites. One common approach is the incorporation of toughening agents, including rubber, thermoplastic polymers, nanoparticles, core-shell particles, and fibers [5–8]. However, introducing these agents into the epoxy matrix comes with its own set of limitations. Achieving compatibility between rubber particles and epoxy resin can be a complex task, potentially leading to suboptimal dispersion or the clustering of rubber particles within the resin, which can reduce their

* Corresponding author.
** Corresponding author. School of Mechanical Engineering, Northwestern Polytechnical University, Xi'an, 710072, PR China.
E-mail addresses: jianjun@nwpu.edu.cn (J. Jiang), d.papageorgiou@qmul.ac.uk (D.G. Papageorgiou).

https://doi.org/10.1016/j.polymer.2024.127065
Received 12 December 2023; Received in revised form 10 April 2024; Accepted 13 April 2024
Available online 15 April 2024

toughening effectiveness. Additionally, simultaneously incorporating both rubber particles and thermoplastic polymers may require trade-offs in mechanical strength or stiffness of the composites [9]. In practice, significant improvements in toughness have been noted when higher quantities of elastomeric or thermoplastic materials are used. For example, achieving a 50 % increase in fracture toughness may require as much as 20 wt% of liquid rubber (LR) [10]. This objective comes with significant challenges, such as the low glass transition temperature (T_g) of LR, which will eventually reduce the highest operating temperature of the structural component manufactured with the rubber-toughened epoxy. Additionally, the use of high LR content presents handling and processing challenges, as it will increase the viscosity of the hybrid system, making more challenging to achieve a homogeneous mixture [11]. Enhancing the toughness of epoxies through the incorporation of rubber or thermoplastic materials often results in a trade-off, leading to reduced thermal stability [12–14] and diminished strength or elastic modulus [15,16]. These compromises significantly constrain the use of epoxy resins in demanding applications that require high thermal and mechanical properties, such as in aerospace components or electronic elements [17]. When it comes to the simultaneous introduction of nanoparticles, issues such as agglomeration or inadequate dispersion pose significant obstacles that can reduce the effectiveness of toughening agents [1,6,18]. In the case of core-shell particles, the synthesis is complex, and the uneven particle size distribution can result in inconsistent toughening effects [19–21]. As for fibers, improper alignment may lead to anisotropic properties, which may not be desirable in certain applications [22–24]. Itis important to note that improving both strength and toughness of an epoxy resin without compromising its thermal stability is very difficult using current design approaches.

Herein, the use of multifunctional nanofillers and a flexible polymer has been proposed to tackle the above issues. The combined contributions of a stiff nanoparticle with a flexible modifier should allow for the simultaneous improvement of both the strength and toughness of epoxy. Previous research has shown that hybrid systems that involve the incorporation of rigid and soft additives, such as polyether amine/graphene oxide (PEA/GO) [25], polyetherimide/carbon nanotube (PEI/CNTs) [1], and polyetherimide/amino groups grafted multiwalled carbon nanotubes (PEI/NH_2-MWCNTs) [26], have demonstrated these benefits. In this study, a novel ternary system has been constructed, comprising of a rigid MXene filler and a toughening agent in the form of pre-polyurethane (PU). MXene nanoplatelets offer unique advantages, as a result of their attractive mechanical, optical, electrical, thermal, and magnetic properties [27]. As a class of transition metal carbides, nitrides, or carbonitrides, MXenes can be synthesized with different transition metals, resulting in a wide range of compositions. Their chemical diversity allows for tailoring the properties of MXenes to meet specific requirements in EP composites, such as enhanced mechanical properties and the preparation of electrically/thermally conductive EP composites. Compared with carbon nanotubes and graphene, MXenes offer flexibility in surface functionalization thanks to their rich surface chemistry that can be modified with various functional groups [28]. Both the tunability in surface functionalization and their hydrophilicity can be utilized to improve dispersion within the epoxy matrix, towards improving interfacial adhesion and enhancing the mechanical properties of the composite. All these parameters render MXenes as very promising candidates for composites reinforcement towards diverse high-end applications. In our case, the $Ti_3C_2T_x$ nanoplatelets, serve as a rigid reinforcement towards improving the strength of the ternary composites.

It is widely recognized that the effectiveness of toughening, whether using flexible or rigid fillers, is significantly influenced by factors such as loading, matrix compatibility and dispersibility [10]. In our research, an approach involving extremely low filler mass-loadings was explored, comprising only 0.05 wt% MXene and 1 wt% PU. It's worth noting that PU, serving as the flexible toughening agent, is the precursor to polyurethane, readily available, and exhibits excellent compatibility with epoxy. Its active isocyanate functional group (-NCO) can chemically bond with the hydroxyl groups (-OH) present in EP, forming strong chemical bonds. Additionally, $Ti_3C_2T_x$ nanoplatelets are terminated with functional groups like –O, –F, and –OH, which enable the formation of hydrogen bonds with –OH groups in the EP matrix, promoting favorable matrix compatibility.

In this study, we established a compatible ternary composite system comprising MXene, PU, and EP. Our goal was to investigate how both flexible and rigid modifiers influence the mechanical properties of the epoxy matrix. We synthesized hydroxyl-terminated MXene nanoplatelets and isocyanate-terminated PU as the primary components that would allow subsequent modifications of the epoxy resin. We then conducted a series of characterizations to establish the quality of the synthesized products before using them. Next, PU and MXene nanoplatelets were incorporated into the epoxy matrix through chemical grafting and blending. Mechanical tests were employed to evaluate their effects on the matrix properties, optimizing the processing parameters to achieve the most favorable modification results. Subsequently, we integrated MXene and PU at optimal loadings to achieve simultaneous improvements in both strength and toughness. Finally, we thoroughly discussed and summarized the underlying reinforcing mechanisms from the hybrid nanocomposites.

2. Materials and methods

2.1. Materials

The IN2 epoxy resin (EP) and AT30 slow epoxy hardener were procured from Easy Composites Ltd. The MAX powder (Ti_3AlC_2) was purchased from Jilin 11 Technology Co., Ltd. Lithium fluoride (LiF), hydrochloric acid (HCl), methylene diphenyl diisocyanate (MDI), and polypropylene glycol (PPG, average M.W. was 425) were bought from Themo Fisher Scientific Co., Ltd. In this paper, PU refers to the pre-polymer of polyurethane.

2.2. Pre-polymerization of polyurethane (PU)

The distillation of PPG was performed prior to synthesis to eliminate any potential residual moisture. Additionally, the reactive glassware, comprising a four-neck flask and a separating funnel, were subjected to desiccation within a vacuum oven at 100 °C to mitigate the harmful impact of moisture. Within the synthesis procedure, an oil bath was used to maintain the temperature at 75 °C and provide the necessary thermal energy, while a measured quantity of PPG was incrementally introduced into the flask in conjunction with MDI, at a weight ratio of MDI to PPG of 1:2. The synthesis of PU proceeded for a duration of 120 min, under a nitrogen atmosphere.

2.3. Synthesis of MXene nanoparticles

The procedure for synthesizing MXene nanoparticles was based on our previous research and is outlined as follows [29,30]. To prepare the etching solution, 20 mL of 9 M hydrochloric acid (HCl) was homogeneously combined with 1.6 g of lithium fluoride (LiF) using magnetic agitation. Subsequently, 1 g of MAX powder was introduced incrementally into the etchant, and stirring was sustained for a period of 24 h at a temperature of 40 °C. Following this step, the resultant reaction product underwent repetitive centrifugation cycles at 3500 revolutions per minute (r/min) for 10 min, followed by thorough washing with deionized water to attenuate any residual acidity until the solution's pH reached 5. Ultrasonication was utilized to achieve the breakdown of multilayered MXene into monolayer or few-layer nanosheets. Subsequently, an additional centrifugation step lasting 60 min at 3500 r/min was carried out to segregate the single/few-layered MXene nanoplatelets from their multi-layered counterparts. Lastly, the MXene slurry underwent freeze-drying to eliminate any moisture.

2.4. Preparation of PU/MXene modified epoxy composites

During the preparation of PU-EP composites, a specified quantity of PU (0.5 wt%, 1 wt%, 2 wt%) was introduced into the epoxy, and subsequently subjected to magnetic stirring at 75 °C for a duration of 60 min to facilitate the reaction between PU and EP. Conversely, for the formulation of MXene-EP composites, the initial step involved the dispersion of the synthesized MXene in ethanol, achieved through ultrasonication over a period of 2 h under ice-bath and in a nitrogen atmosphere. The DGEBA epoxy resin, having been pre-dissolved in acetone, was then combined with the MXene/ethanol suspension. The MXene nanoplatelet loadings were selected as 0.03 wt%, 0.05 wt%, and 0.1 wt%. To create the PU-MXene-EP composites, the preparation processes used for PU-EP and MXene-EP composites were carried out in a sequential manner and then combined to produce the final ternary MXene-PU-EP composites. A schematic illustration of the preparation process is presented in Fig. S2 of the supporting information. The solvent removal was conducted via magnetic stirring at 70 °C for 180 min before mixing the PU-MXene-EP with the curing agent, at a mass ratio of 10:3. After that, the degassing of epoxy blends was executed under vacuum followed by casting into the mould as well as curing at 60 °C for 60 min. The mechanism for the preparation of MXene-PU-EP composite is illustrated in Fig. 1. During the polymerization process of PU, the excessive MDI reacted with PPG and the obtained PU product was terminated by –NCO groups. After that, chemical grafting took place between PU and EP and the –OH groups of EP reacted with –NCO groups of PU to get the PU-EP composite, with PU chains grafted onto EP. Thereafter, the MXene nanoplatelets were mixed with PU-EP in the solvent and the hydrogen linkages were constructed between oxygen containing groups such as urethane bonds and –OH in EP as well as –F, –O, –OH groups in MXene nanoplatelets.

2.5. Characterization

The morphological characteristics of the MXenes were examined utilizing both a scanning electron microscope (SEM, InspectTM FEI, Netherlands) and a transmission electron microscope (TEM, Tecnai FEI, USA). The changes in peak patterns of MXene nanoplatelets during the synthesis were studied using X-ray diffraction (XRD, PANalytical, Netherlands). The surface chemical composition and structure of the MXene were analyzed through X-ray photoelectron spectroscopy (XPS, ThermoFisher Nexsa). Furthermore, the structure of the synthesized MXene was verified by employing a Raman spectroscope (Renishaw inViaTM). The Raman signal was collected by using a 785 nm edge laser with a grating of 1200 grooves/min at a laser power of 1 %. Differential Scanning Calorimetry (DSC) tests were performed by using a TA Instruments DSC25, and the instrument cell was purged with constant flow (50 mL/min) of N_2, with ramping rates of 10 °C/min.

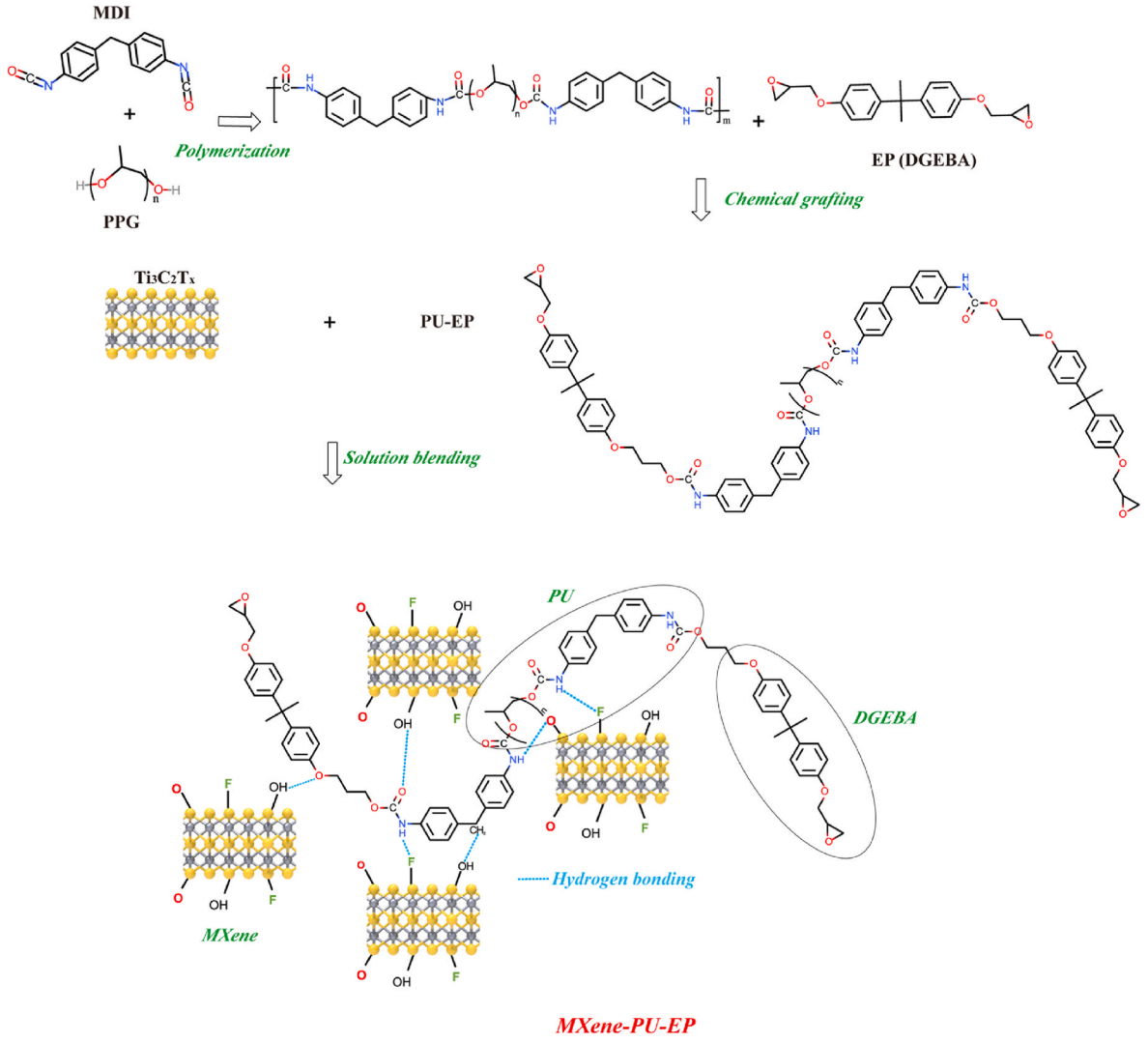

Fig. 1. Synthesis process and reaction mechanism for the formation of MXene-PU-EP ternary composites.

Thermogravimetric analysis (TGA) was carried out using a Thermogravimetric Analyzer TGA 5500 from TA Instruments. Tensile and three-point bending tests were executed using a universal testing machine (Instron, 68TM-10), in accordance with the standards set forth by ASTM D638 and ASTM D790. Five specimens were tested for each set of samples, at a loading rate of 2 mm/min. Fracture toughness evaluation was conducted in accordance with the ASTM D5045 standard, employing a three-point bending pre-cracked configuration. The specimen size was 40 mm × 8 mm × 4 mm and the span was set as 32 mm. The fracture toughness K_{IC} was calculated according to the following formula [31]:

$$K_{IC} = \frac{P_Q}{BW^{1/2}} f(x), W = 2B$$

$$f(x) = 6x^{1/2} \frac{1.99 - x(1-x)(2.15 - 3.93x + 2.7x^2)}{(1-2x)(1-x)^{3/2}}, x = \frac{a}{W}$$

where K_{IC} is the fracture toughness, $f(x)$ is the shape factor, P_Q is the peak load, B and W are the specimen thickness and width respectively, and a is the crack length.

3. Results and discussion

3.1. Structure and morphology of MAX phase and MXene nanoplatelets

Figs. 2(a) and 1(b) show the SEM and TEM images of the synthesized MXene nanoplatelets. In Fig. 2(a), the SEM image reveals the distinctive accordion-like morphology of MXene, while Fig. 2 (b) displays a thin MXene nanosheet. Comparative analyses were carried out between MAX and MXene using XRD and Raman spectroscopy. As depicted in Fig. 2(c), the (002) peak exhibited a noticeable shift from the initial 9.58° in MAX to 6.81° in MXene, indicating an expanded layer spacing from 0.92 nm to 1.3 nm. Additionally, the absence of the (104) peak at 39° in the MXene XRD spectrum indicated the complete removal of the aluminum (Al) element [32]. Regarding the Raman spectra presented in Fig. 2(d), the presence of two separate peaks at 200 cm^{-1} and 725 cm^{-1}, as opposed to MAX element, provides further confirmation of the successful synthesis of MXene nanoplatelets [33]. Collectively, these findings validate the successful fabrication of MXene nanoplatelets.

3.2. Primary characterization of PU-EP composites

The progress of the PU polymerization and PU-EP grafting reactions was monitored using Fourier-transform infrared spectroscopy (FTIR) (Fig. 3(a)) and proton nuclear magnetic resonance spectroscopy (^{1}H NMR) (Fig. 3(b) and Fig. S1). Initially, the primary components, MDI and PPG, displayed prominent peaks at 2273 cm^{-1} and 3450 cm^{-1}, corresponding to the N–C═O and O–H stretching vibrations, respectively. After the reaction was complete, the intensity of N–C═O groups in the PU was reduced due to the polymerization between N–C═O in MDI and O–H in PPG. As for EP resin, the peak at 914 cm^{-1} corresponds to the epoxy ring structure and the band at 3450 cm^{-1} revealed the O–H vibration mode. The weak O–H signal in EP was due to the uncured epoxy monomer, a result of the absence of a curing reaction between the epoxy and the amine groups within the curing agent [34]. In addition, the obtained PU and PU-EP exhibited distinct peaks at around 1727 cm^{-1} and 3300 cm^{-1}, which were attributed to the C═O and N–H bonds, indicating the formation of urethane bonds. Following the chemical grafting between PU and EP, the resulting PU-EP composite showed the absence of the N–C═O vibration peak, indicating a thorough reaction between the N–C═O groups of PU and the O–H groups of EP. This conclusion was further supported by the ^{1}H NMR analysis of PU in

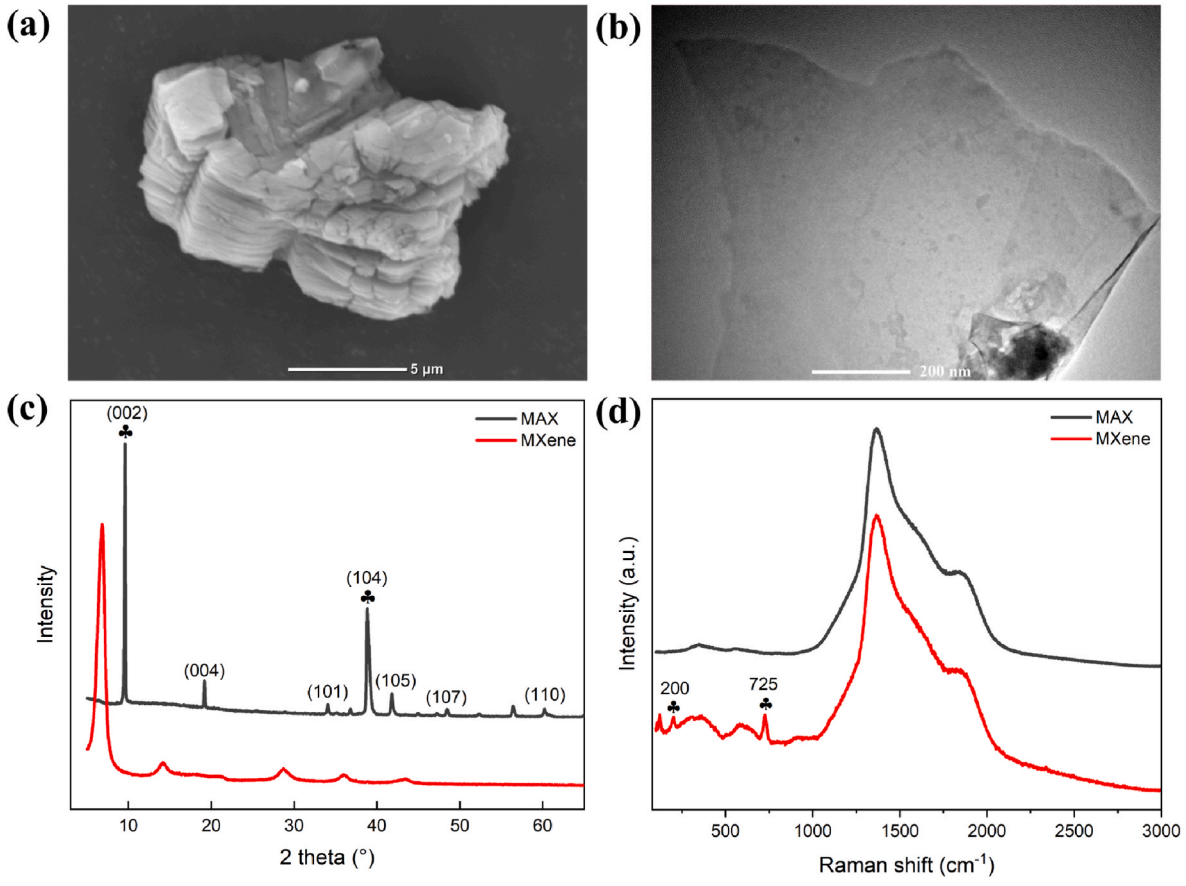

Fig. 2. (a–b) The SEM and TEM images of the synthesized MXene; (c–d) XRD and Raman curves comparison of MAX phase and MXene nanoplatelets.

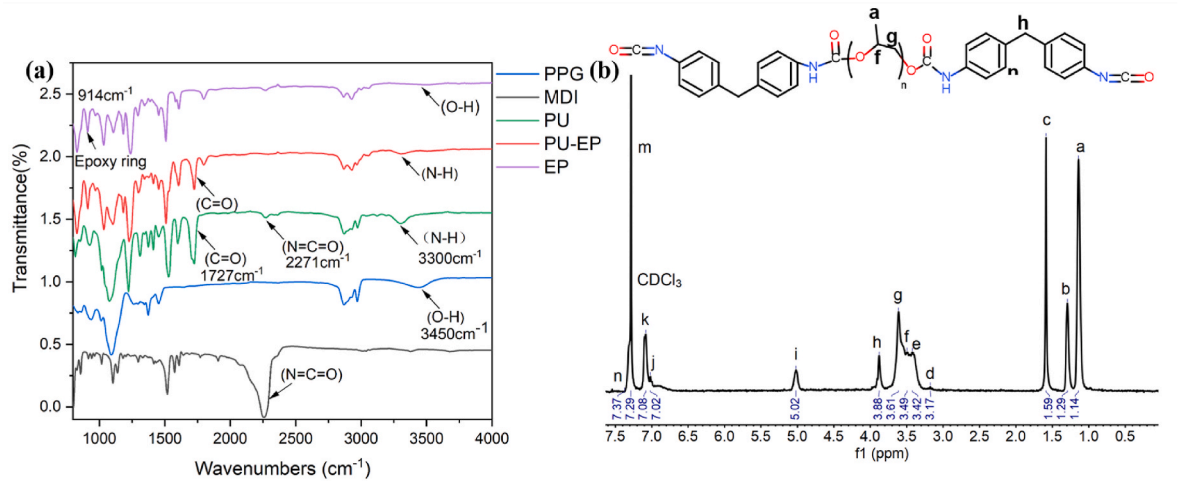

Fig. 3. (a) FTIR spectra of the MDI, PPG chemicals and the synthesized PU, EP as well as PU-EP composite; (b) ^{1}H NMR spectra of PU polymer.

$CDCl_3$, as shown in Fig. 3(b). The strongest peak m at 7.29 ppm represented the $CDCl_3$. And the resonances at 7.08 ppm (peak k) and 7.37 ppm (peak n) were assigned to the protons of benzene rings adjacent to –NH–(C═O)–O, while the peaks at 1.14 ppm, 3.61 ppm and 3.49 ppm were attributed to the hydrogen in $–CH_3$, $–CH(CH_3)$-, and $–CH_2$- from the PPG segment [35,36]. Moreover, the appearance of chemical shifts at 7.02 ppm that corresponded to the amine protons of the urethane linkage further supported the successful synthesis of PU [36]. The ^{1}H NMR analysis of MDI, PPG, and PU-EP is provided in the Supplementary Information, see Figs. S1, 2, 3.

3.3. Elemental composition of MXene/PU-EP composites surface

X-ray photoelectron spectroscopy (XPS) analysis was conducted to provide insights into the structural composition and elemental changes before and after the introduction of MXene and PU into EP. As shown in

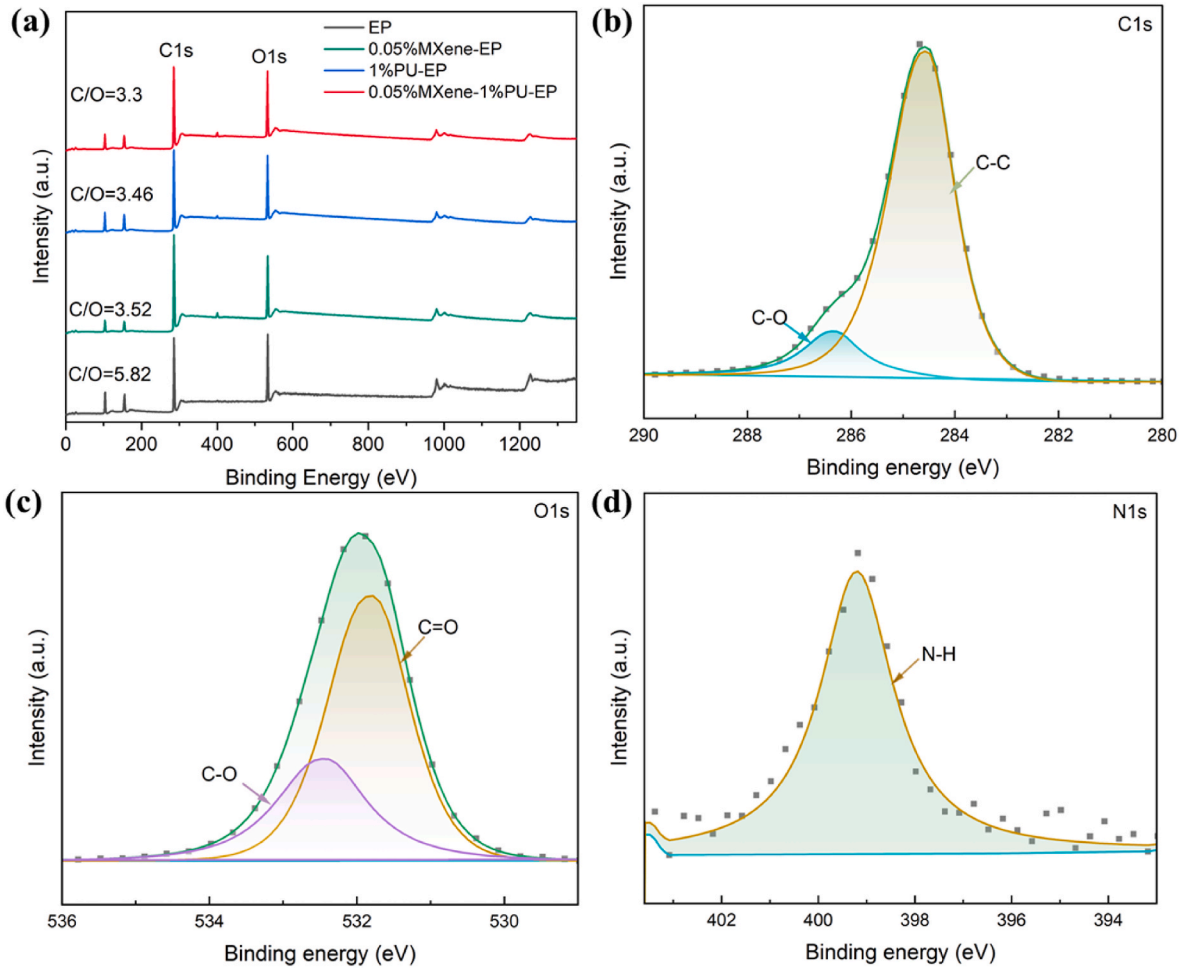

Fig. 4. (a) XPS wide-scan spectra; (b–d) C1s, O1s, N1s spectra of 0.05 % MXene-1%PU-EP.

Fig. 4(a), oxygen and carbon are the predominant elements in the EP-related composites. Notably, the C/O ratio exhibits a significant decrease from the initial value of 5.82 for unmodified EP to 3.52 for 0.05 % MXene-EP, 3.46 for 1 % PU-EP, and 3.3 for 0.05 % MXene-1% PU-EP. This change is attributed to the presence of functional groups (-O, –OH) from MXene and (-NCO, –O═C–O) from PU, confirming the successful modification of EP by MXene and PU fillers.

Regarding the C1s spectrum in Fig. 4(b), the peaks centered at approximately 284.6 eV and 286.3 eV correspond to the C–C and C–O bonds, respectively. In the O1s spectrum presented in Fig. 4(c), the binding energies at 531.6 eV and 532.4 eV are associated with C═O and C–O species. In the N1s spectrum, a single peak appeared at 399 eV, indicating the presence of N–H bonding, consistent with the incorporation of PU into EP. Consequently, the decreased C/O ratios and the presence of N–H bonds collectively confirm the successful integration of MXene and PU within EP matrix.

3.4. Thermal properties of hybrid MXene/PU-EP composites

DSC and TGA tests were performed to assess the effect of MXene and PU on the thermal characteristics of epoxy resin. As illustrated in Fig. 5 (a), the glass transition temperature (T_g) of the EP was determined to be 64 °C, and a slight increase to 65.5 °C was observed when incorporating 0.05 % MXene-EP. This increase in T_g can be ascribed to the increased crosslinking density and/or chain nanoconfinement effects that arise from the integration of MXene nanoparticles into the epoxy resin matrix [26]. In the case of the 0.05 % MXene-1%PU-EP composite, it displayed a slightly-increased glass transition temperature (T_g) of 64.7 °C when compared to the unmodified EP of 64 °C, which might originate from the fact that the concentration of the modifier was too small to severely alter the T_g, and the weak thermal stability of PU might have negated the improved glass transition temperature that was expected as a result of the hydrogen bonds formed between MXene, PU, and EP [37–39]. Overall, the incorporation of MXene and PU at low concentrations in the EP formulation did not lead to a reduction in the T_g; instead, they exhibited slightly higher or comparable T_g values in comparison to the unaltered EP.

The TGA results presented in Fig. 5(b) reveal that the thermal stability was increased from EP to 0.05 % MXene-EP and 0.05 % MXene-1% PU-EP composites. Correspondingly, the onset of significant weight loss (Temperature at 5 % mass loss, T_{d5}) commenced at approximately 313 °C, 316 °C, and 324 °C, as depicted in the inset figure. It can be inferred that the addition of MXene nanoplatelets and PU increased the onset temperature of decomposition, signifying that the synthesized MXene/PU-modified epoxy composites did not compromise their thermal stability. This observation can be explained by the following factors: (i) the inclusion of PU and MXene resulted in chemical grafting and hydrogen bonding with the epoxy, increasing the cross-linking density and consequently delaying the decomposition process [40]; (ii) the high aspect ratio of MXene nanoparticles served as a barrier, hindering the release of small gaseous molecules and thereby contributing to improved thermal stability [41]. The results presented above illustrate that both the 0.05 % MXene-EP and 0.05 % MXene-1% PU-EP composites exhibit improved thermal stability when compared to the unmodified epoxy resin.

3.5. Tensile properties of MXene/PU-EP composites

The stress-strain curves, illustrating the tensile properties of MXene/PU-EP composites, are presented in Fig. 6. In the MXene-EP composites, which include various very low mass fractions of MXene nanoparticles ranging from 0, 0.03 %, 0.05 %, 0.075 % and 0.1 wt%, a pattern of initial improvement followed by subsequent decline is evident, as depicted in Fig. 6(a) and (b). Consequently, the composite containing 0.05 wt% MXene nanoplatelets demonstrates the highest tensile strength at 83.4 MPa, along with the highest Young's modulus at 3725 MPa. This represents increases of 21 % and 20 % compared to the EP composite, which displayed respective values of 69.1 MPa and 3125 MPa. The decrease in tensile performance observed with the further addition of MXene fillers may be attributed to agglomeration phenomena. The agglomeration and re-stacking of MXene flakes were prone to take place, particularly in the high-viscosity epoxy environment [42]. This, in turn, could lead to the formation of a weak interface between the aggregated MXenes and the epoxy resin, resulting in significant stress concentration [43,44].

In the case of the PU-modified EP composites, as depicted in Fig. 6(c) and (d), the highest tensile strength of 87.2 MPa is achieved when the PU loading is 1 wt%, representing a significant 26 % enhancement compared to the neat EP composite. The strengthening mechanism behind these phenomena could be ascribed in combination to the strong chemical bonding and the enhanced chemical compatibility between PU and EP, which led to a more defined and optimized network structure with higher crosslinking density, contributing to better interfacial adhesion [45]. Also, the possible intermolecular hydrogen bonding between the hydroxyl group in EP and isocyanate group in PU and the interpenetrating polymer network played a positive role in enhancing the tensile properties [46]. Moreover, the anchoring and bridging effects of MXenes and the ability of the PU phase to dissipate stress concentration and absorb energy during plastic deformation, contributing to improved overall tensile strength.

Crucially, the introduction of both MXene and PU fillers into the EP matrix yielded an enhancement in tensile properties. The mechanical reinforcement achieved by the hybrid system, which combines MXene

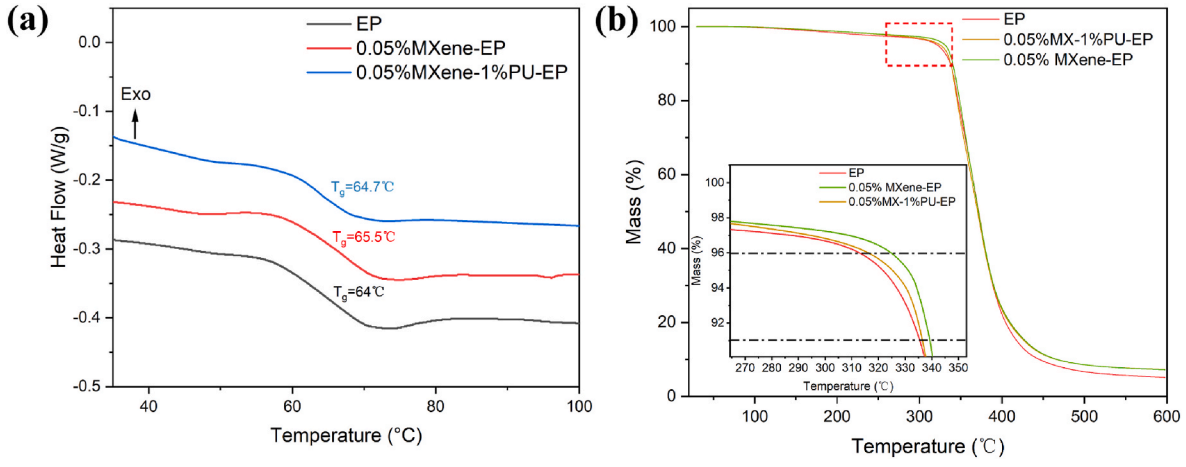

Fig. 5. (a) DSC and (b) TGA curves comparison between EP, 0.05%MXene-EP, and 0.05%MXene-1%PU-EP.

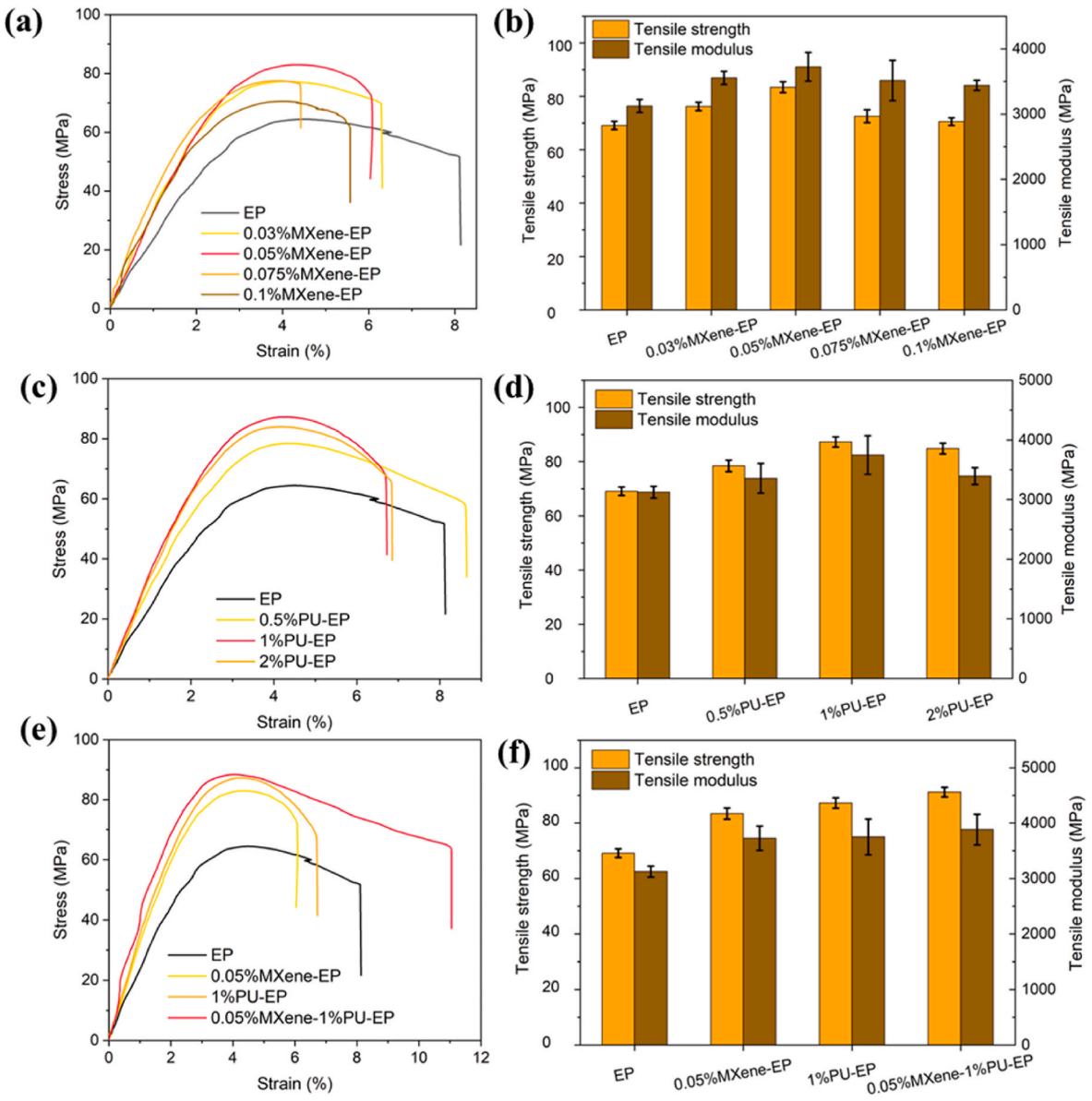

Fig. 6. Representative stress-stain curves (a, c, e) and corresponding strength and Young's (tensile) modulus results (b, d, f) for MXene-EP, PU-EP, and MXene-PU-EP composites.

and PU, exceeded the maximum improvements attained by the individual MXene-EP and PU-EP composites [47,48]. As shown in Fig. 6(e) and (f), the optimal tensile strength of 91.2 MPa is attained with a remarkable 32 % improvement over EP when the filler loadings of MXene and PU are set at only 0.05 wt% and 1 wt%, respectively. Additionally, both Young's modulus and elongation at break undergo significant improvements, with corresponding increases of 24 % (from 3125 MPa to 3883 MPa) and 37 % (from 8 % to 11 %). These substantial enhancements can be attributed to the combinatory effects of MXene and PU, where they respectively serve as the rigid filler and flexible component, simultaneously enhancing both strength and toughness.

3.6. *Flexural properties of MXene/PU-EP composites*

A series of comparative experiments were carried out to evaluate the influence of MXene and PU modifiers on the flexural properties of EP composites. As shown in Fig. 7(a and b), when using MXene fillers with a mass fraction below 0.05 %, there were slight improvements in flexural strength, increasing from 113.2 MPa for EP to 133.3 MPa for 0.03 wt% MXene-EP and 143.7 MPa for 0.05 wt% MXene-EP. However, the introduction of additional MXene nanoparticles at 0.075 % and 0.1 % mass fractions resulted in a gradual decrease in strength, with values decreasing by 15 % and 13 %, respectively, compared to 0.05 wt% MXene-EP. As the MXene nanoparticles loading increased gradually, they were more inclined to agglomerate and create stress-concentrated areas, promoting the initiation and propagation of cracks until eventual failure. In the case of the PU-EP composites, as depicted in Fig. 7(c and d), an optimal loading of 1 wt% PU resulted in significant improvements in bending strength, reaching 155.5 MPa, and in flexural modulus, reaching 4014 MPa. These enhancements represent respective increases of 37 % and 46 % when compared to the pristine EP composite, attributed to crack anchoring and plastic deformation effects [49]. The isocyanate groups of PU can react with the hydroxyl and amine groups within the epoxy resin to form a network of strong covelent bonds as shown in Fig. 2, which enhance resistance to cracking, ultimately contributing to increased flexural modulus and strength. Similarly, as observed in Fig. 7(e and f), the 0.05 % MXene-1% PU-EP composite demonstrates the highest flexural strength of 165.7 MPa and flexural

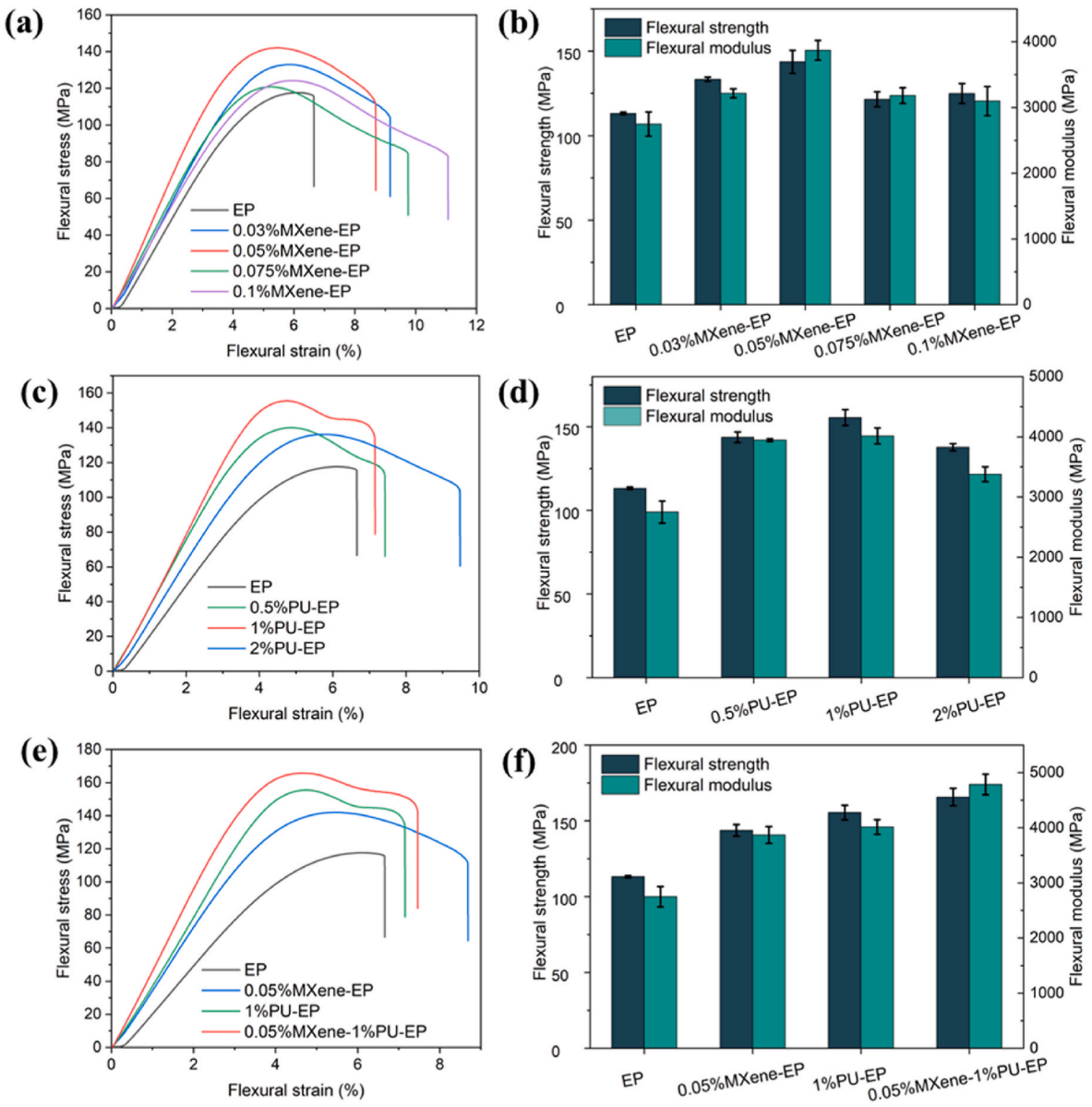

Fig. 7. Representative flexural stress-stain curves (a, c, e) and corresponding strength and flexural modulus results (b, d, f) for MXene-EP, PU-EP, and MXene-PU-EP composites.

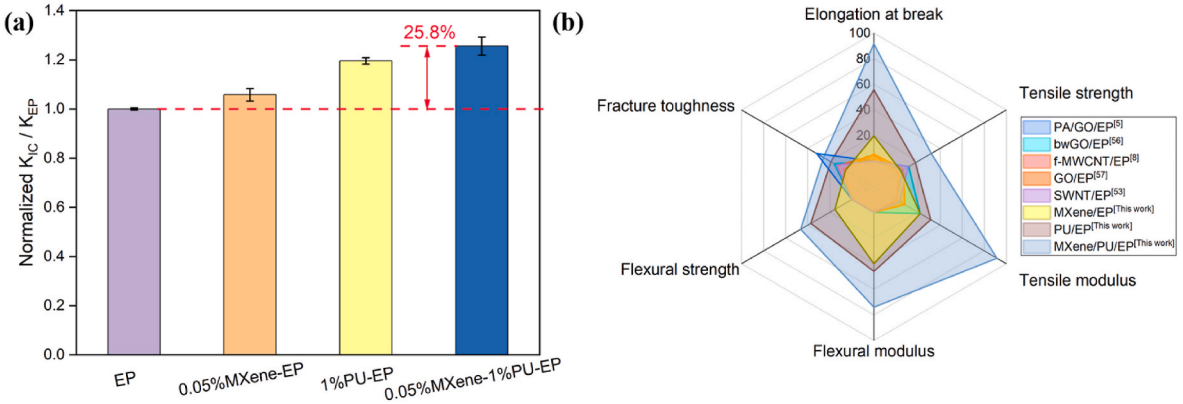

Fig. 8. (a) Normalized fracture toughness results for MXene/PU modified EP composites; (b) Comparison of % improvements in tensile/flexural strength and modulus, elongation at break and fracture toughness among various epoxy composites.

modulus of 4785 MPa. These values represent improvements of 46 % and 74 % respectively when compared to the unmodified EP and they align with consistent tensile performance.

3.7. Fracture toughness of MXene/PU-EP composites

The fracture toughness of the ternary composites was assessed through single-edge-notch three-point-bending experiments. The adoption of a normalized analytical approach facilitated direct comparability and representation among different composite materials, irrespective of their geometric configurations and loading conditions [50,51]. The results of the normalized fracture toughness (n-K_{IC}), in relation to the MXene/PU modified epoxy resin composites compared to the unmodified epoxy resin, are presented in Fig. 8(a). The unaltered epoxy resin demonstrated a normalized K_{IC} value of 1.0. In accordance with prior findings from tensile and flexural analyses, loadings of 0.05 wt% and 1 wt% were determined as the optimal filler concentrations for MXene and PU, respectively. The 0.05 % MXene-EP composite demonstrated an elevated **n-K_{IC}** value of 1.058, signifying a 5.8 % increase relative to pure EP, which might be ascribed to crack anchoring and bridging effects delay or prevent propagation of cracks [52]. Furthermore, the 1 % PU-EP composite displayed a 19.5 % enhancement, resulting in an *n-K_{IC}* value of 1.195. This improvement is linked to the increased ductility that is a characteristic of thermoplastic materials [11]. Notably, the combination of MXene and PU yielded a remarkable *n-K_{IC}* value of 1.258, representing a notable 25.8 % increment over the pristine EP thanks to toughening effects from both MXene and PU. Considering the results discussed herein, our current approach, which involves the simultaneous incorporation of both MXene and PU, has proven its effectiveness in enhancing the strength and toughness of a brittle epoxy resin. Importantly, our research has demonstrated significant improvements in the strength and fracture toughness of EP composites, surpassing findings reported in existing literature, as summarized in Table 1, with some notable examples shown in Fig. 8(b).

Table 1
A comparison of the mechanical properties of epoxy matrix composites as reported in the literature.

Specimen	Tensile strength increase (%)	Young's modulus increase (%)	Fracture toughness increase (%)	Reference
SWNT/EP	11	3	14	[53]
p-SWCNT/EP	16	18	4	[54]
f-SWCNT/EP	17	26	18	[54]
DWCNT-NH_2/EP	−0.5	6.3	18.4	[55]
f-MWCNT/EP	2	1	13	[8]
BNNS/EP	2.8	4	14.7	[8]
CNT/EP	0	4	5	[8]
PA/GO/EP	−1.8	−1.1	8.4	[5]
bwGO/EP	4.2	12	10.8	[56]
GO/EP	7	8	8	[57]
MXene/EP	4.5	22	5.8	This work
PU/EP	17.5	31.5	19.1	This work
MXene/PU/EP	32	91.5	25.8	This work

SWNT (single wall carbon nanotube); p-SWCNT (pristine SWCNT); f-SWCNT (PAMAM-0 functionalized SWCNTs); DWCNT-NH_2 (double-wall carbon nanotubes with amino-groups); f-MWCNT (nitric acid treated multi-walled carbon nanotubes); BNNS (boron nitride nanosheets); bwGO (base-washed graphene oxide).

3.8. Evaluation of the interfacial strengthening mechanism of MXene/PU-EP composites by fractography

A crack propagation model was proposed to illustrate the underlying mechanisms of MXene and PU in enhancing the mechanical performance of EP. The post-mortem fracture surfaces of MXene/PU/EP composites were analyzed by SEM. As shown in Fig. 9(a) and (g), after tensile testing, the fracture cross-section of unmodified EP displayed primarily straight crack propagation paths with sharp crack tips, indicating its inherent brittle fracture characteristics. After chemical grafting with PU, the fracture mode transitioned into a feather-like ductile pattern, characterized by a disordered surface morphology and interrupted, deflected crack propagation routes, as evidenced in Fig. 9(b–c) and (h). Upon the introduction of MXene nanosheets into the EP matrix, the fracture surface exhibited increased coarseness and greater irregularities, as depicted in Fig. 9(d). This phenomenon was attributed to the crack-pinning and anchoring effect of MXenes, where the progression of cracks was hindered by the presence of MXene obstacles, resulting in multiple instances of crack termination and deflection. The 0.05 % MXene-1% PU-EP composite, with both MXene and PU incorporated, exhibited a fracture surface that demonstrated enhanced toughening. It not only displayed feather-like ductile characteristics but also demonstrated a substantial anchoring effect due to the presence of MXenes, effectively restraining crack propagation (Fig. 9(e and f)). Furthermore, MXene nanosheets facilitated the bridging of PU-EP segments through hydrogen bonding, further impeding crack extension, as demonstrated in Fig. 9(i).

In summary, the integration of MXene and PU in a carefully balanced composition ratio played a pivotal role in improving both the strength and toughness of EP. This improvement was accomplished through mechanisms involving plastic deformation, chemical bonding between PU and EP, as well as the anchoring and bridging effects of MXenes.

4. Conclusions

This study introduced an innovative approach involving the simultaneous incorporation of a flexible modifier, thermoplastic polyurethane (PU), and a rigid component, MXene nanoparticles, to enhance both the strength and toughness of the inherently brittle epoxy (EP) matrix. The ternary system comprising MXene/PU/EP exhibited cohesion facilitated by chemical bonding and hydrogen interactions among PU, MXene, and EP. After a series of systematic refinements, the 0.05 % MXene-1% PU-EP composite emerged as the optimal formulation, resulting in a significant improvement in the mechanical properties of EP. Specifically, the modified EP composite demonstrated a 32 % increase in tensile strength, a 46 % increase in flexural strength, and a 25.8 % increase in fracture toughness when compared to unmodified EP. These enhancements can be attributed to the toughness provided by thermoplastic PU, strengthened by robust chemical bonding between PU and EP, as well as the crack-anchoring and bridging effects imparted by MXene nanoplatelets. Importantly, this work achieved the toughening and strengthening of epoxy with minimal additions of 0.05 wt% MXene and 1 % PU, all while preserving its thermal stability. The small dosage of fillers undoubtedly paves the way for the widely application of robust advanced materials that are exceptionally strong and tough, as well as low-cost. Such materials hold immense potential across a wide spectrum of industries, including manufacturing and construction, where the need for durable, strong and resilient components is paramount. Furthermore, these improvements are particularly valuable in high-performance composites for the aerospace and automotive sectors, enabling the development of lighter, stronger, and tougher thus more reliable materials to enhance the efficiency and safety of critical applications in these industries.

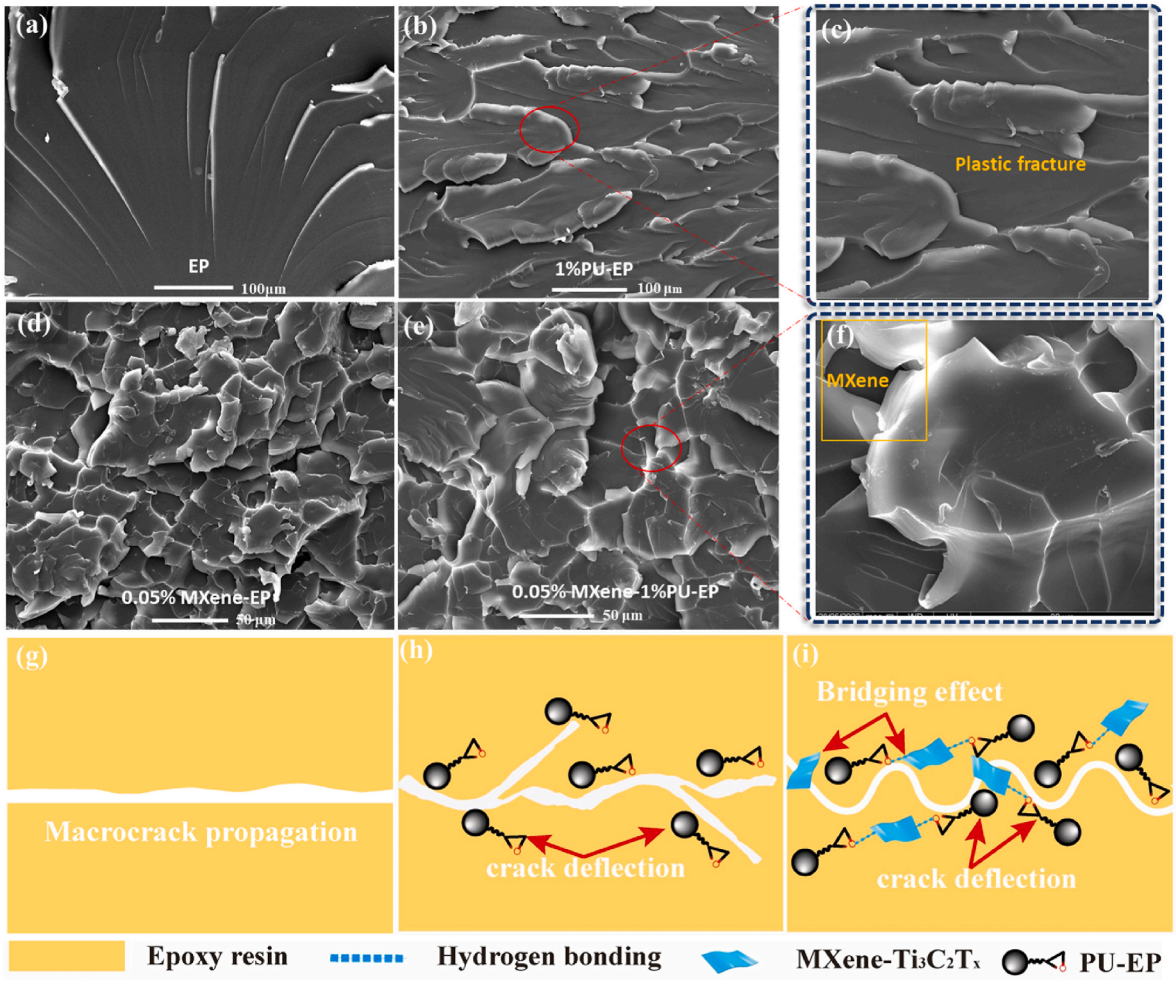

Fig. 9. SEM images of tensile fracture cross-section: (a) EP; (b–c) 1%PU-EP; (d) 0.05 % MXene-EP; (e–f) 0.05 % MXene-1%PU-EP; Schematic of crack propagation path and the corresponding strengthen mechanisms for: (g) EP; (h) 1%PU-EP; (i) 0.05 % MXene-1%PU-EP.

CRediT authorship contribution statement

Yi Hu: Writing – original draft, Visualization, Methodology, Investigation, Formal analysis, Conceptualization. **Junzhen Chen:** Investigation. **Guoyu Yang:** Investigation. **Yujun Li:** Investigation. **Ming Dong:** Investigation. **Qi Li:** Investigation. **Hongna Yuan:** Investigation. **Han Zhang:** Writing – review & editing, Resources. **Nicola M. Pugno:** Writing – review & editing. **Jianjun Jiang:** Supervision, Resources. **Dimitrios G. Papageorgiou:** Writing – review & editing, Writing – original draft, Supervision, Resources, Investigation, Funding acquisition, Conceptualization.

Declaration of competing interest

We declare that we have no financial and personal relationships with other people or organizations that can inappropriately influence our work, there is no professional or other personal interest of any nature or kind in any product, service and/or company that could be constructed as influencing the position presented in, or the review of, the manuscript entitled.

Data availability

Data will be made available on request.

Appendix A. Supplementary data

Supplementary data to this article can be found online at https://doi.org/10.1016/j.polymer.2024.127065.

References

[1] H. Ma, M.A. Aravand, B.G. Falzon, Synergistic enhancement of fracture toughness in multiphase epoxy matrices modified by thermoplastic and carbon nanotubes, Compos. Sci. Technol. (2021) 201.
[2] D. Li, E. Peng, F. Lu, B.L. Wang, Y.B. Shen, P.X. Liu, et al., Toughing epoxy nanocomposites with graphene-encapsulated liquid metal framework, Chem. Eng. J. 455 (2023).
[3] M.Y. Khalid, A. Kamal, A. Otabil, O. Mamoun, K. Liao, Graphene/epoxy nanocomposites for improved fracture toughness: a focused review on toughening mechanism, Chem. Eng. J. Adv. 16 (2023).
[4] K. Yang, S.J. Wu, J. Guan, Z.Z. Shao, R.O. Ritchie, Enhancing the mechanical toughness of epoxy-resin composites using natural silk reinforcements, Sci. Rep. 7 (2017).
[5] X. Zhao, Y. Li, W. Chen, S. Li, Y. Zhao, S. Du, Improved fracture toughness of epoxy resin reinforced with polyamide 6/graphene oxide nanocomposites prepared via in situ polymerization, Compos. Sci. Technol. 171 (2019) 180–189.
[6] N. Domun, H. Hadavinia, T. Zhang, T. Sainsbury, G.H. Liaghat, S. Vahid, Improving the fracture toughness and the strength of epoxy using nanomaterials - a review of the current status, Nanoscale 7 (23) (2015) 10294–10329.
[7] X.Q. Mi, N. Liang, H.F. Xu, J. Wu, Y. Jiang, B. Nie, et al., Toughness and its mechanisms in epoxy resins, Prog. Mater. Sci. 130 (2022).
[8] N. Domun, K.R. Paton, H. Hadavinia, T. Sainsbury, T. Zhang, H. Mohamud, Enhancement of fracture toughness of epoxy nanocomposites by combining nanotubes and nanosheets as fillers, Materials 10 (2017).
[9] N. Zheng, Y.D. Huang, H.Y. Liu, J.F. Gao, Y.W. Mai, Improvement of interlaminar fracture toughness in carbon fiber/epoxy composites with carbon nanotubes/polysulfone interleaves, Compos. Sci. Technol. 140 (2017) 8–15.

[10] T.Q. Li, S.Y. He, A. Stein, L.F. Francis, F.S. Bates, Synergistic toughening of epoxy modified by graphene and block copolymer micelles, Macromolecules 49 (24) (2016) 9507–9520.
[11] T.T. Wang, P. Huang, Y.Q. Li, N. He, S.Y. Fu, Epoxy nanocomposites significantly toughened by both poly(sulfone) and graphene oxide, Compos. Commun. 14 (2019) 55–60.
[12] R. Bagheri, B.T. Marouf, R.A. Pearson, Rubber-toughened epoxies: a critical review, Polym. Rev. 49 (3) (2009) 201–225.
[13] U. Farooq, J. Teuwen, C. Dransfeld, Toughening of epoxy systems with interpenetrating polymer network (IPN): a review, Polymers 12 (9) (2020).
[14] L. Zhou, Y.W. Fu, T. Yin, Z.Y. Luo, Synergetic effect of epoxy resin and carboxylated nitrile rubber on tribological and mechanical properties of soft paper-based friction materials, Tribol. Int. 129 (2019) 314–322.
[15] L. Tao, Z.Y. Sun, W. Min, H.W. Ou, L.L. Qi, M.H. Yu, Improving the toughness of thermosetting epoxy resins blending triblock copolymers, RSC Adv. 10 (3) (2020) 1603–1612.
[16] Z.Y. Sun, L. Xu, Z.G. Chen, Y.H. Wang, R. Tusiime, C. Cheng, et al., Enhancing the mechanical and thermal properties of epoxy resin via blending with thermoplastic polysulfone, Polymers 11 (3) (2019).
[17] X.Q. Wang, B. Ma, K. Wei, W.J. Zhang, Thermal stability and mechanical properties of epoxy resin/microcapsule composite phase change materials, Construct. Build. Mater. 312 (2021).
[18] S. Liu, V.S. Chevali, Z.G. Xu, D. Hui, H. Wang, A review of extending performance of epoxy resins using carbon nanomaterials, Compos. B Eng. 136 (2018) 197–214.
[19] N. Ning, W.S. Liu, Q.L. Hu, L.Y. Zhang, Q.R. Jiang, Y.P. Qiu, et al., Impressive epoxy toughening by a structure-engineered core/shell polymer nanoparticle, Compos. Sci. Technol. (2020) 199.
[20] D. Quan, A. Ivankovic, Effect of core-shell rubber (CSR) nano-particles on mechanical properties and fracture toughness of an epoxy polymer, Polymer 66 (2015) 16–28.
[21] S.R. Mousavi, S. Estaji, M.R. Javidi, A. Paydayesh, H.A. Khonakdar, M. Arjmand, et al., Toughening of epoxy resin systems using core-shell rubber particles: a literature review, J. Mater. Sci. 56 (33) (2021) 18345–18367.
[22] N.Q. Nguyen, M. Mehdikhani, I. Straumit, L. Gorbatikh, L. Lessard, S.V. Lomov, Micro-CT measurement of fibre misalignment: application to carbon/epoxy laminates manufactured in autoclave and by vacuum assisted resin transfer moulding, Compos. Appl. Sci. Manuf. 104 (2018) 14–23.
[23] H. Zhang, K.F. Wu, G.M. Xiao, Y.X. Du, G.H. Tang, Experimental study of the anisotropic thermal conductivity of 2D carbon-fiber/epoxy woven composites, Compos. Struct. 267 (2021).
[24] A. Parmiggiani, M. Prato, M. Pizzorni, Effect of the fiber orientation on the tensile and flexural behavior of continuous carbon fiber composites made via fused filament fabrication, Int. J. Adv. Des. Manuf. Technol. 114 (7–8) (2021) 2085–2101.
[25] J. Fan, Z.J. Wang, J.P. Yang, X.B. Yin, Y.F. Zhao, Applying alternating "rigid-and-soft" interphase into functionalized graphene oxide/epoxy nanocomposites toward enhanced mechanical properties, Appl. Surf. Sci. 585 (2022).
[26] Z.G. Chen, J. Luo, Z. Huang, C.Q. Cai, R. Tusiime, Z.Y. Li, et al., Synergistic toughen epoxy resin by incorporation of polyetherimide and amino groups grafted MWCNTs, Compos. Commun. 21 (2020).
[27] X. Jiang, A.V. Kuklin, A. Baev, Y. Ge, H. Agren, H. Zhang, et al., Two-dimensional MXenes: from morphological to optical, electric, and magnetic properties and applications, Phys. Rep.-Rev. Section Phys. Lett. 848 (2020).
[28] Y. Hu, G. Yang, J. Chen, Y. Li, M. Dong, H. Zhang, et al., Interfacial engineering of hybrid MXene-Ni-CF tri-core–shell composites for electromagnetic interference shielding and E-heating applications, Compos. Appl. Sci. Manuf. 178 (2024) 107990.
[29] Y. Hu, S.J. Pang, G.Y. Yang, X.M. Yao, C.B. Li, J.J. Jiang, et al., MXene modified carbon fiber composites with improved mechanical properties based on electrophoretic deposition, Mater. Res. Bull. 150 (2022).
[30] Y. Hu, S. Pang, J. Li, J. Jiang, D.G. Papageorgiou, Enhanced interfacial properties of hierarchical MXene/CF composites via low content electrophoretic deposition, Compos. B Eng. 237 (2022) 109871.
[31] J. Kim, J. Cha, B. Chung, S. Ryu, S.H. Hong, Fabrication and mechanical properties of carbon fiber/epoxy nanocomposites containing high loadings of noncovalently functionalized graphene nanoplatelets, Compos. Sci. Technol. 192 (2020).
[32] L. Wang, L.X. Chen, P. Song, C.B. Liang, Y.J. Lu, H. Qiu, et al., Fabrication on the annealed Ti3C2Tx MXene/Epoxy nanocomposites for electromagnetic interference shielding application, Compos. B Eng. 171 (2019) 111–118.
[33] A. Sarycheva, Y. Gogotsi, Raman spectroscopy analysis of the structure and surface chemistry of Ti3C2Tx MXene, Chem. Mater. 32 (8) (2020) 3480–3488.
[34] M. Sabu, E. Bementa, Y. Jaya Vinse Ruban, S. Ginil Mon, A novel analysis of the dielectric properties of hybrid epoxy composites, Adv. Compos. Hybrid Mater. 3 (3) (2020) 325–335.
[35] M.L. Polo, M.E. Spontón, F. Jaramillo, D.A. Estenoz, G.R. Meira, Linear segmented polyurethanes: I. A kinetics study, J. Appl. Polym. Sci. 135 (4) (2018).
[36] T. Saito, Y. Aizawa, K. Tajima, T. Isono, T. Satoh, Organophosphate-catalyzed bulk ring-opening polymerization as an environmentally benign route leading to block copolyesters, end-functionalized polyesters, and polyester-based polyurethane, Polym. Chem. 6 (24) (2015) 4374–4384.
[37] H. Liu, M. Liu, P. Zhang, K. Xue, T. Yao, L. Liu, et al., POSS-polyurethane prepolymer strengthened and toughened CF/epoxy resin composites for room and simulated Arctic ambient temperature, Polymer 294 (2024) 126692.
[38] L. Papadopoulos, N.M. Malitowski, A. Zamboulis, S. Friebel, D. Bikiaris, T. Robert, Influence of bio-based 2,5-furandicarboxylic acid on the properties of water-borne polyurethane dispersions, React. Funct. Polym. 190 (2023) 105622.
[39] M. Kluge, D.N. Bikiaris, T. Robert, Enhancing the properties of poly(propylene succinate) by the incorporation of crystallizable symmetrical amido diols, Eur. Polym. J. 120 (2019) 109195.
[40] Y.Q. Li, D.Y. Pan, S.B. Chen, Q.H. Wang, G.Q. Pan, T.M. Wang, In situ polymerization and mechanical, thermal properties of polyurethane/graphene oxide/epoxy nanocomposites, Mater. Des. 47 (2013) 850–856.
[41] B.Y. Chen, N. Ma, X. Bai, H.M. Zhang, Y. Zhang, Effects of graphene oxide on surface energy, mechanical, damping and thermal properties of ethylene-propylene-diene rubber/petroleum resin blends, RSC Adv. 2 (11) (2012) 4683–4689.
[42] J. Wang, C.-F. Du, Y. Xue, X. Tan, J. Kang, Y. Gao, et al., MXenes as a versatile platform for reactive surface modification and superior sodium-ion storages, Exploration 1 (2) (2021) 20210024.
[43] M.S. Chang, An investigation on the dynamic behavior and thermal properties of MWCNTs/FRP laminate composites, J. Reinforc. Plast. Compos. 29 (24) (2010) 3593–3599.
[44] Y.X. Zhou, F. Pervin, L. Lewis, S. Jeelani, Experimental study on the thermal and mechanical properties of multi-walled carbon nanotube-reinforced epoxy, Mater. Sci. Eng. 452 (2007) 657–664.
[45] A. Kieffer, A. Hartwig, Interphase reaction of isocyanates with epoxy resins containing functional groups of different reactivity, Macromol. Mater. Eng. 286 (4) (2001) 254–259.
[46] S.-J. Park, J.-S. Jin, Energetic studies on epoxy–polyurethane interpenetrating polymer networks, J. Appl. Polym. Sci. 82 (3) (2001) 775–780.
[47] B. Pradhan, S.K. Srivastava, Synergistic effect of three-dimensional multi-walled carbon nanotube-graphene nanofiller in enhancing the mechanical and thermal properties of high-performance silicone rubber, Polym. Int. 63 (7) (2014) 1219–1228.
[48] Y.M. Jen, J.C. Huang, K.Y. Zheng, Synergistic effect of multi-walled carbon nanotubes and graphene nanoplatelets on the monotonic and fatigue properties of uncracked and cracked epoxy composites, Polymers 12 (9) (2020).
[49] S.Q. Deng, L. Djukic, R. Paton, L. Ye, Thermoplastic-epoxy interactions and their potential applications in joining composite structures - a review, Compos. Appl. Sci. Manuf. 68 (2015) 121–132.
[50] L.C. Tang, H. Zhang, J.H. Han, X.P. Wu, Z. Zhang, Fracture mechanisms of epoxy filled with ozone functionalized multi-wall carbon nanotubes, Compos. Sci. Technol. 72 (1) (2011) 7–13.
[51] N. Shirodkar, S.F. Cheng, G.D. Seidel, Enhancement of Mode I fracture toughness properties of epoxy reinforced with graphene nanoplatelets and carbon nanotubes, Compos. B Eng. (2021) 224.
[52] S. Chandrasekaran, N. Sato, F. Tölle, R. Mülhaupt, B. Fiedler, K. Schulte, Fracture toughness and failure mechanism of graphene based epoxy composites, Compos. Sci. Technol. 97 (2014) 90–99.
[53] M.A. Rafiee, J. Rafiee, Z. Wang, H. Song, Z.-Z. Yu, N. Koratkar, Enhanced mechanical properties of nanocomposites at low graphene content, ACS Nano 3 (12) (2009) 3884–3890.
[54] L. Sun, G.L. Warren, J.Y. O'Reilly, W.N. Everett, S.M. Lee, D. Davis, et al., Mechanical properties of surface-functionalized SWCNT/epoxy composites, Carbon 46 (2) (2008) 320–328.
[55] F.H. Gojny, M.H.G. Wichmann, U. Köpke, B. Fiedler, K. Schulte, Carbon nanotube-reinforced epoxy-composites: enhanced stiffness and fracture toughness at low nanotube content, Compos. Sci. Technol. 64 (15) (2004) 2363–2371.
[56] Z. Li, R.G. Wang, R.J. Young, L.B. Deng, F. Yang, L.F. Hao, et al., Control of the functionality of graphene oxide for its in epoxy nanocomposites application, Polymer 54 (23) (2013) 6437–6446.
[57] Y.J. Wan, L.C. Tang, L.X. Gong, D. Yan, Y.B. Li, L.B. Wu, et al., Grafting of epoxy chains onto graphene oxide for epoxy composites with improved mechanical and thermal properties, Carbon 69 (2014) 467–480.